LIMNOLOGY and OCEANOGRAPHY

ASLO

Limnol. Oceanogr. 71, 2026, e70436

doi: 10.1002/lno.70436

RESEARCH ARTICLE

Eco-morphodynamic response of deltaic salt marshes to successive extreme storms

Jie Wang [1,2], Ming Shi,[2] Zhijun Dai [2*], Huan-Feng Duan,[1] Xuefei Mei,[2] Wen Wei,[3] Jiejun Luo [2], Weihua Li,[2] Sergio Fagherazzi[4]

[1]State Key Laboratory of Climate Resilience for Coastal Cities, Department of Civil and Environmental Engineering, The Hong Kong Polytechnic University, Hong Kong, China; [2]State Key Laboratory of Estuarine and Coastal Research, East China Normal University, Shanghai, China; [3]School of Ocean Engineering and Technology, Sun Yat-Sen University/ Southern Marine Science and Engineering Guangdong Laboratory (Zhuhai), Zhuhai, China; [4]Department of Earth and Environment, Boston University, Boston, Massachusetts, USA

Abstract

Deltaic salt marshes deliver crucial ecosystem services, including wave and flooding attenuation, making them key components of coastal nature-based solutions. However, their sustainability under climate change remains poorly understood, particularly regarding cumulative impacts from successive extreme weather events in regions with declining fluvial sediment supply. Here, we investigate the recovery capacity of deltaic salt marshes following successive extreme storms. We leverage in-situ data on intertidal hydrodynamics, bed elevation changes, and marsh vegetation dynamics, collected during typhoon and cold wave events in the East Chongming Wetland, the largest open tidal wetland in the Changjiang (Yangtze) Delta, China. Our results demonstrate that both typhoons and cold waves enhanced intertidal hydrodynamic forcing (inundation depth, wave energy, and tidal currents) and suspended sediment concentrations in vegetated areas, resulting in mean net bed erosion of 2.98 and 4.82 cm, respectively. The total salt marsh area decreased by 15.7% (from 7.05×10^5 to 5.94×10^5 m^2) after the storms, with fragmentation increasing 50.8% between 2022 and 2023. Elevation-dependent responses generated two distinct bands of alongshore marsh erosion and vegetation loss. Cold waves caused particularly severe impacts through combined hydromechanical stress and belowground tissue damage from rapid temperature cooling. These findings reveal compounding stressors from sequential extreme hydrometeorological events that threaten the recovery of exposed salt marshes, providing critical insights for nature-based coastal protection and disaster adaptation strategies.

Deltaic tidal wetlands are critical landforms where fluvial and marine dynamics interact dynamically, providing important ecological services such as sediment trapping, land-building, and storm protection (Kirwan and Megonigal 2013). Salt marshes with dense stems and leaves can dampen waves and tidal energy, thereby stabilizing intertidal substrates, and thus are utilized as a primary nature-based defense against coastal storms (Borsje et al. 2011; Temmerman et al. 2023). However, in recent decades, basin-derived sediments have been trapped by dams, reducing fluvial sediment supply to many deltas that support salt marsh survival against accelerated sea level rise (Dethier et al. 2022; Murray et al. 2022). In addition, increasingly frequent extreme meteorological and hydrological events, for instance, tropical cyclones and cold waves, have triggered profound impacts on the health and sustainability of salt marshes (Morton and Barras 2011; Kim et al. 2020). In some regions, these disturbances can impair the recovery capacity of coastal wetlands and threaten the medium- and long-term protective efficacy of coastal green-gray infrastructures; whereas in other areas, storms nourish coastal marsh ecosystems by delivering additional marine sediments (Stagg and Mendelssohn 2011; Q. Zhu and Wiberg 2022; Wang et al. 2025). Therefore, it is critical to explore how extreme storms affect salt marshes in sediment-deficient deltas, possibly reducing the effectiveness of nature-based solutions.

*Correspondence: zjdai@sklec.ecnu.edu.cn

Associate editor: Ruth Reef

Intertidal vegetation structure varies with bed elevation, and vegetated and unvegetated zones respond differently to external disturbances (Silvestri et al. 2005). In particular, storm-induced effects in salt marshes generally depend on storm track and intensity, intertidal surficial sediment properties, topographic slope, vegetation species, and marsh extension (Cahoon 2006; Morton and Barras 2011; Leonardi et al. 2018). Turner et al. (2006) reported that about 131×10^6 t of inorganic sediments were deposited by Hurricanes Katrina and Rita in 2005, which made direct landfall in the Mississippi Delta and adjacent coastal wetlands, accounting for 12% of the annual suspended sediment supply. In contrast, other studies have shown that extreme storms can induce net sediment export, cliff erosion, and salt marsh loss, especially at marsh margins exposed to intense wave forcing (Bendoni et al. 2016; Rupprecht et al. 2017). In addition, in many regions aboveground vegetation senesces in winter; thus, seasonal meteorological disturbances can have different eco-morphodynamic effects on salt marshes due to shifts in the physical protection effectiveness of the vegetation canopy (Callaghan et al. 2010; WinklerPrins et al. 2024). Without salt marsh vegetation, low-resistance intertidal areas release more suspended sediment during winter cold waves (Coulombier et al. 2012; Kim et al. 2020). Dzimballa et al. (2025) highlighted that seasonal hydrodynamic conditions and windows of vegetation growth also regulate the long-term development of salt marshes, which is important for intertidal geomorphic stability and ecological restoration. Hence, salt marsh phenology interacts with storm occurrence, altering the interannual trajectory of tidal wetlands in the delta.

Most studies focus on a single storm, and little is known about how successive extreme events, defined as two or more storms occurring within the same summer-autumn or winter season, or across both seasons within a given year, affect marsh interannual recovery capacity and stability. The 1st storm may only partially compromise the health of the salt marsh vegetation through hydromechanical effects, for instance, by breaking, uprooting, or washing away vegetation, and eroding the vegetation boundary (Friedrichs and Perry 2001; Morton and Barras 2011). If subsequent storms strike before the marsh has fully recovered or in the absence of salt marsh protection, overall damage is likely to be amplified (Cahoon 2006). Thus, cascading disturbances triggered by successive storms can not only cause more severe geomorphic changes and marsh loss but also substantially impact subsequent marsh recovery (Z. Zhu et al. 2020; Temmerman et al. 2023). Furthermore, short-term disturbances can affect deltaic intertidal eco-morphodynamics over longer time scales. If successive extreme storms push salt marsh ecosystems beyond their survival thresholds, intertidal geomorphic stability and coastal protection will decline, especially when combined with inadequate fluvial sediment input and sea level rise (Fagherazzi et al. 2020). Typically, a greater elevation difference between the bare flat and the salt marsh can trigger accelerated lateral erosion, and these adverse effects can be amplified by storms (Willemsen et al. 2022). Thus, widespread intertidal bed scours and sediment export in both vegetated and unvegetated areas, driven by successive storms, will substantially restrict salt marsh expansion and sediment accretion and diminish its ecosystem services.

Open-coast salt marshes developing on sloping shores are more vulnerable to erosion by extreme storms because of the direct impact of wind waves. In contrast, in sheltered salt marshes such as in the Venice Lagoon (Italy) and in the Virginia Coast Reserve (USA), the primary effect of coastal storms may be sedimentation (Q. Zhu and Wiberg 2022; Tognin et al. 2025). Moreover, in narrow salt marshes, wave erosion may dominate during storm events, whereas in extensive marshes, erosion is concentrated mainly at marsh edges, while resuspended bed sediments tend to be deposited within the higher marsh interior. Major knowledge gaps persist in the eco-morphodynamic response of narrow, open-coast salt marshes to successive extreme storms. Notably, the overall ability of salt marsh ecosystems to attenuate waves and tidal flows and stabilize shorelines reaches its annual minimum in winter. If strong cold waves strike during this period, the erosion vulnerability of deltaic tidal wetlands will be amplified. Therefore, systematic analyses of how cross-seasonal extreme storm sequences affect the eco-morphodynamic responses and recovery capacity of open-coast and narrow salt marshes in sediment-deficient deltas are needed.

The Changjiang (Yangtze) Delta is one of the world's largest fluvial-tidal deltas, with three orders of distributaries and 4 mouths formed over the past 2000 yr (Fig. 1a,b) (Chen et al. 1988). The East Chongming Wetland is one of the fastest prograding tidal wetlands in the Changjiang Delta and is subjected to extreme storms almost every year (Fig. 1b) (Yun 2004). The most recent coastal defense project, combining flood-defense seawalls, intertidal reclamation, and salt marsh restoration, was completed in 2016 in the northern East Chongming Wetland (Fig. 1c,d) (Ge et al. 2019). Along this open coast, typhoons in summer and autumn (Supporting Information Fig. S1) and cold waves in winter can directly impact the salt marshes, thus making it an ideal site to examine the effects of successive storms on open-coast salt marshes and their recovery over time. We hypothesize that: (1) The impact of different types of extreme storms strongly depends on seasonal timing and salt marsh phenology and (2) Successive storms will reduce marsh interannual recovery capacity, thus threatening marsh ecosystem services. Our findings reveal how deltaic tidal wetlands respond to successive extreme storm events, helping improve nature-based coastal solutions for climate change.

Materials and methods

Geographical setting of the study area

Large amounts of terrigenous sediments have historically accumulated in the Changjiang Delta, forming extensive tidal

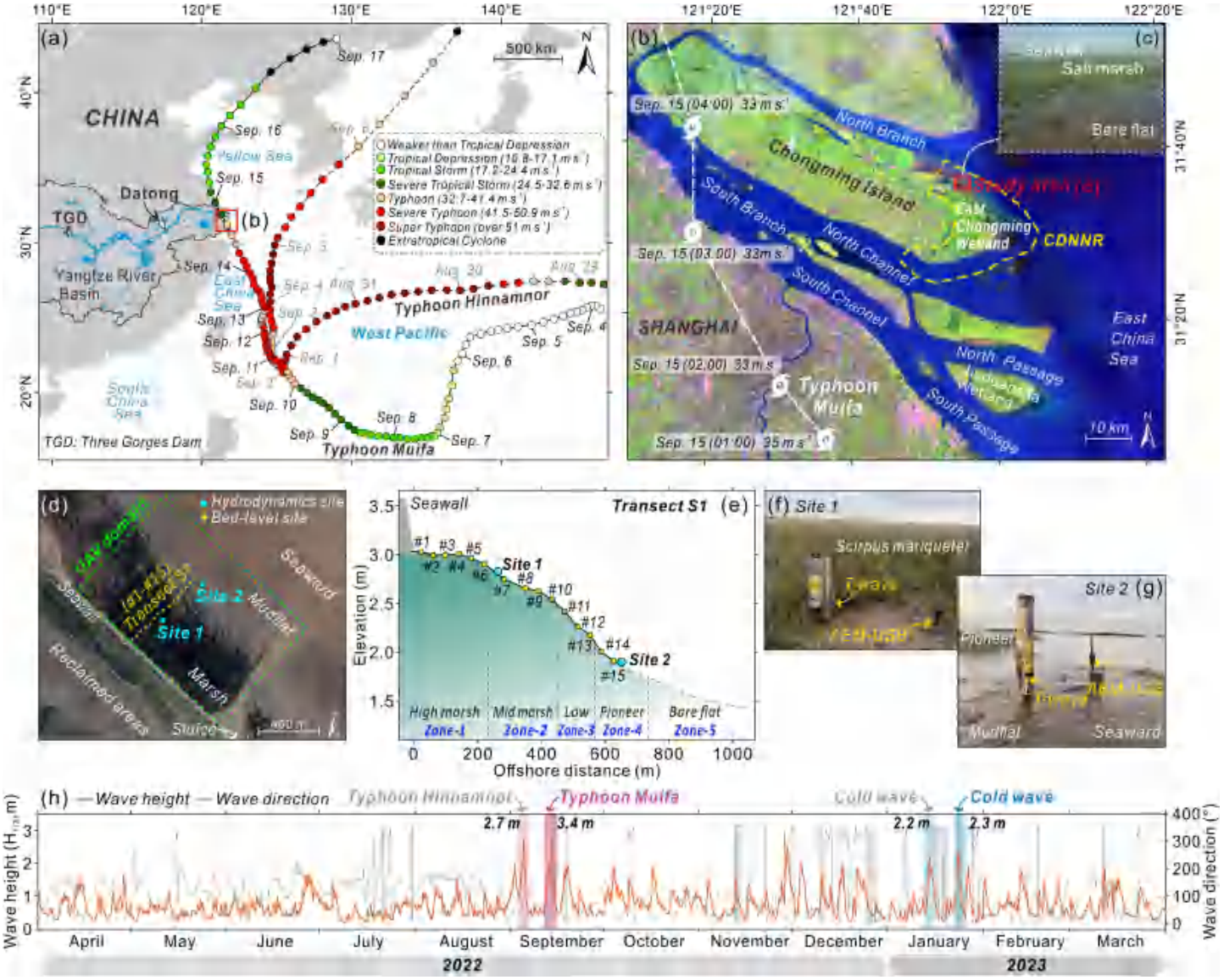

Fig. 1. Maps of the study area and in-situ observation sites. (a) Track and intensity of Typhoons Hinnamnor and Muifa, which originated in the western Pacific Ocean on August 29, 2022 and September 4, 2022, respectively. (b) Landfall of Muifa in the Changjiang Delta, with wind speeds up to 35 m s^{-1}. Location of the East Chongming Wetland, Chongming Dongtan National Nature Reserve (CDNNR), and the study area are indicated. (c) Unmanned aerial vehicle (UAV)–acquired imagery of the study area. (d) Deployment configuration of the two intertidal hydrodynamic instruments and 15 bed elevation monitoring sites along Transect S1; the UAV survey domain is delineated. (e) Topographic profile along Transect S1; the studied intertidal zone was divided into five subzones: high marsh (Zone 1), mid marsh (Zone 2), low marsh (Zone 3), pioneer marsh (Zone 4), and bare flat (Zone 5). (f, g) Photographs of deployed T-wave and AEM-USB, collecting wind waves and tidal current data. (h) Time series of significant wave height ($H_{1/3}$) and direction from April 2022 to March 2023 were acquired from the ERA5. Two typhoons and two cold waves occurred during the study period.

flats (Chen et al. 1988). However, the annual fluvial sediment load of the Changjiang River has declined by 70% since the 1980s due to upstream damming (Dai et al. 2018; Mei et al. 2023). The studied area in the open-coast East Chongming Wetland lies on the seaward side of a new dike (Supporting Information Text S1; Fig. 1b–d). The native S. mariqueter germinates in April, reaches full growth by August, and senesces in winter (Li et al. 2014; Yuan et al. 2020). In this study, the intertidal zone was divided into five sub-zones depending on bed elevation, topographic slope, and marsh growth characteristics (Silvestri et al. 2005; Yang et al. 2020). The zones are: high marsh (Zone 1), mid marsh (Zone 2), low marsh (Zone 3), pioneer marsh (Zone 4), and bare flat (Zone 5) (Fig. 1e).

Extreme storms in the Changjiang Delta

The Changjiang Delta lies at the interface between the East Asian continent and the northwestern Pacific Ocean and is therefore highly vulnerable to land-sea meteorological disturbances. Two extreme typhoons struck the Changjiang Delta in the summer of 2022. Typhoon Hinnamnor originated from the northwestern Pacific on August 28, 2022, passing within 300 km of the East Chongming Wetland and bringing winds up to 55 m s^{-1} (Fig. 1a; Supporting Information Text S2). The nearshore significant wave height increased to 2.7 m (Fig. 1h). Typhoon Muifa formed on September 4, 2022, and made landfall on September 15 (Fig. 1a,b). The nearshore significant wave height rose to 3.4 m (Fig. 1h). In addition, two cold waves hit the Changjiang Delta in the subsequent winter. During field observations, widespread water freezing was observed in intertidal ponds and low-lying areas, and some salt marsh roots were exposed.

Data acquisition of intertidal hydrodynamics

We collected intertidal hydrodynamic data, including water depth, wave height, tidal flow velocity, and suspended sediment concentration (SSC) at two locations, Site 1 in the mid marsh and Site 2 in the pioneer marsh (Fig. 1d–g). In the summer of 2022, hydrodynamic data at both sites were collected from September 7 to 18, covering the Typhoon Muifa (Supporting Information Text S3). Observations for the winter of 2022 were conducted from December 21 to 26. In addition, during the 2nd cold wave, only water depth and wave data were recorded at both sites from January 23 to 25 (Fig. 2). Intertidal water depth and significant wave height ($H_{1/3}$) data were measured using a fixed TWave-101 instrument (Linkocean, China) (Wei et al. 2022) (Fig. 1f–g). The 2D velocities of tidal currents were measured with the electromagnetic current meter AEM-USB (ALEC, Japan) (Shi et al. 2025). Water turbidity was measured using the Optical Backscatter Sensor OBS-3A (Campbell Scientific, Canada).

Based on the acquired water depths, waves, and tidal currents, we subsequently calculated the bed shear stresses induced by tidal currents (τ_c, N m^{-2}) and waves (τ_w, N m^{-2}) (Supporting Information Text S4) (van Rijn 1993; Whitehouse 2000; Soulsby and Clarke 2005). Finally, the combined wave-tidal bed shear stresses (τ_{cw}, N m^{-2}) were computed with Eq. 1 (Soulsby 1995):

$$\tau_{cw} = \tau_c \left[1 + 1{:}2 \left(\frac{\tau_w}{\tau_c + \tau_w} \right)^{3{:}2} \right] \quad (1)$$

Measurement of intertidal bed elevations

Monthly bed elevations at 15 fixed stations along the monitoring transect S1 were measured using a GPS-RTK device (iRTK5X, Hi-Target, China) (Supporting Information Text S5). The iRTK5X measures the spatial coordinates using Global Navigation Satellite System and Real-Time Kinematics (RTK) techniques. In total, intertidal bed elevations were measured seven times from July 2022 to June 2023, and these data were then used to analyze bed erosion and deposition magnitudes under various hydrodynamic conditions.

Unmanned aerial vehicle surveys and vegetation parameters

We measured the density and height of salt marsh vegetation in July 2022. A total of six sample plots (25 × 25 cm) were placed evenly from the high marsh to the pioneer vegetation (Supporting Information Fig. S4) (Shi et al. 2025). To monitor marsh dynamics in the East Chongming Wetland, we employed a Unmanned Aerial Vehicle (UAV) (Phantom 4 RTK, DJI, China) equipped with a high-precision visible-light single-lens to acquire large-scale images of intertidal areas (Supporting Information Text S6) (Liang et al. 2024). A total of three UAV-based surveys were conducted in the East Chongming Wetland on August 14, 2022 (before Typhoon Hinnamnor and Muifa), April 8, 2023 (after two cold waves), and August 16, 2023 (during the peak of the growing season).

We then divided the UAV domain into a 20 × 20 m grid, comprising 64 alongshore and 42 cross-shore cells, for a total of 106 cells (Fig. 6). Two indices (the Coverage Index and Landscape Shape Index [LSI]) were calculated for each cell of the grid to quantify and characterize spatial patterns of salt marsh vegetation (Eqs. 2, 3) (Remmel and Csillag 2003):

$$\text{Covreage}_{marsh} = A_{marsh} = A_{grid} \quad (2)$$

$$\text{LSI}_{marsh} = 0{:}25\, E_{marsh} = \sqrt{A_{marsh}} \quad (3)$$

where A_{grid} is the area of the whole grid (m^2), A_{marsh} is the total area of all marsh patches in a grid (m^2), and E_{marsh} is the total length of all marsh patch boundaries (m).

Statistical analysis

To compare intertidal hydrodynamic differences between regular tidal and storm conditions, arithmetic means and corresponding standard deviations of maximum wave height ($H_{1/3}$), current velocities and SSCs of flood/ebb tidal flows were calculated at two monitoring sites. Comparisons between two sites were performed using a t-test. For the 15 intertidal elevation monitoring sites, 5 statistical metrics (minimum, 1st quartile, median, 3rd quartile, maximum) were computed over four periods (i.e., Typhoon Muifa, 2nd cold wave, February to June 2023, and the entire study period). In addition, Pearson correlation analyses were carried out to quantify linear correlations between changes in intertidal bed elevation and marsh coverage/LSI, with a 0.05 alpha threshold regarded as statistically significant.

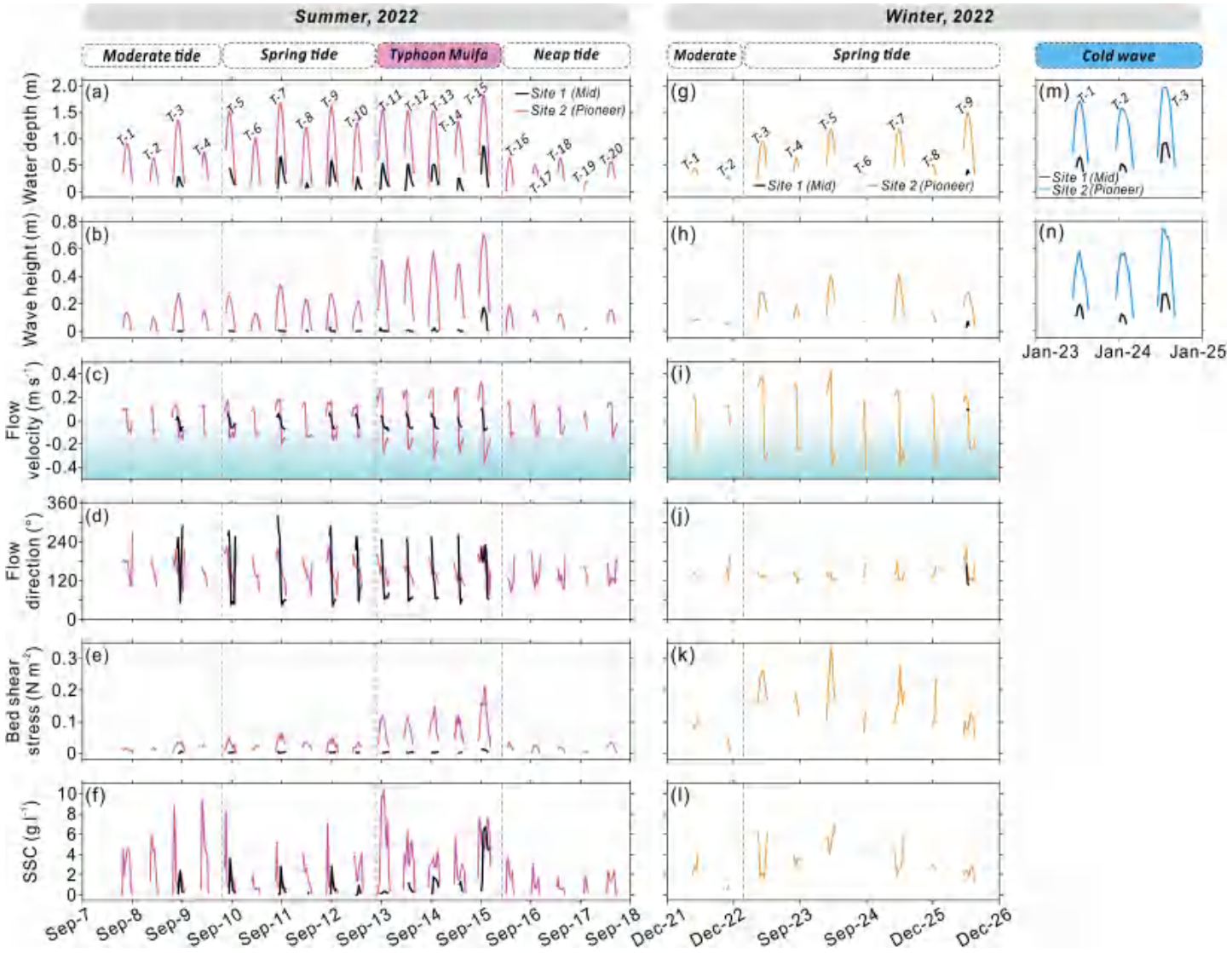

Fig. 2. Intertidal hydrodynamic regimes in the East Chongming Wetland under contrasting forcing scenarios. (a–f) Time series of observed water depth, significant wave height ($H_{1/3}$), tidal flow velocity and direction, combined wave-current bed shear stress, and suspended sediment concentration (SSC) at Site 1 (mid marsh) and Site 2 (pioneer marsh) during summer 2022 (September 7–18). Typhoon Muifa impacted the study area from September 13 to 15. (g–n) Observed intertidal hydrodynamics during winter 2022, encompassing the 2nd cold wave.

Results

Intertidal hydrodynamics during typhoons in summer

The inundation depth at the marsh edge (Site 2) was greater than that in the mid marsh (Site 1), and the maximum water depths rose to 1.84 and 0.86 m, respectively, during Typhoon Muifa (Fig. 2a). Significant wave heights ($H_{1/3}$) exhibited similar variation patterns to water depths; the maximum significant wave height in the pioneer marsh increased from 0.34 m during spring tide to 0.71 m during Typhoon Muifa (Fig. 2b). Wave forcing in the mid marsh remained weak, with a maximum value during Muifa of 0.16 m, due to the dissipative effect of the 400-m-wide salt marsh (Fig. 2b). Velocities of ebb and flood currents in the pioneer marsh were larger than those in the mid marsh. During Typhoon Muifa, the mean flood and ebb velocities at Site 2 reached 24.74 ± 4.53 and 22.33 ± 6.04 cm s^{-1}, respectively, which were 97.9% and 69.1% faster than those during spring tides (Fig. 3b,c; Supporting Information Table S1). Tidal flow directions at the two sites differed markedly. During spring tides and Typhoon Muifa, the flow direction in the pioneer marsh was primarily Southeast to East-southeast, parallel to the direction of the marsh edge and seawall (Fig. 2d; Supporting Information Fig. S5a). In contrast, tidal flow direction at the mid marsh was mainly Northeast and East-northeast, oriented perpendicular to the dike (Supporting Information Fig. S5b). Such directional shifts from pioneer to mid marsh indicate that tidal currents were deflected as they propagated through the salt marshes.

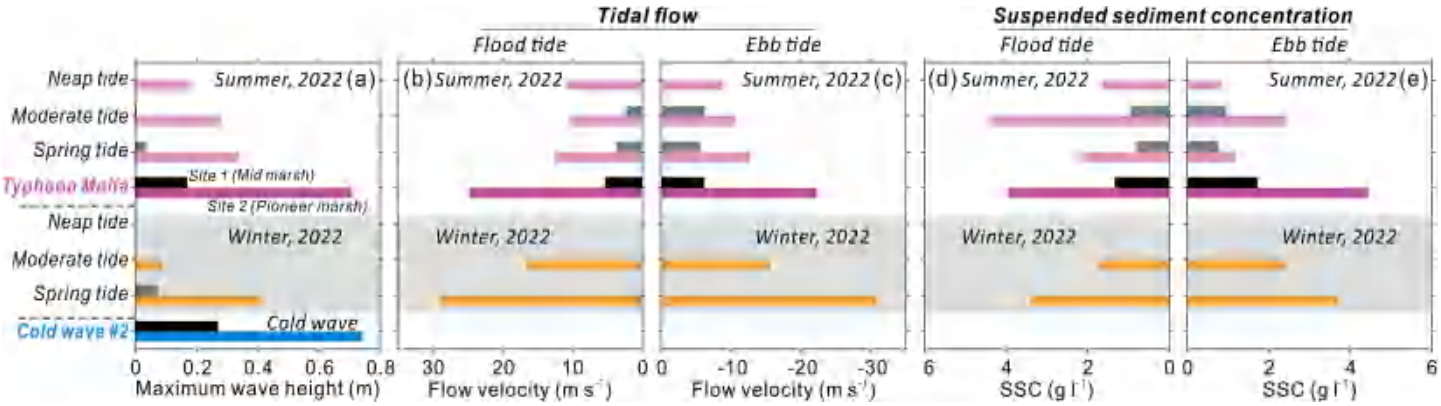

Fig. 3. Comparisons of mean intertidal hydrodynamic parameters, (a) maximum significant wave height ($H_{1/3}$), (b, c) mean flow velocity, and (d, e) mean suspended sediment concentration (SSC) during flood and ebb, at two sites during neap/spring tides and extreme storms.

The maximum combined wave-current bed shear stress in the pioneer marsh increased from 0.07 N m^{-2} during spring tides to 0.21 N m^{-2} during Typhoon Muifa (Fig. 2e). During the initial observation period, the SSC of neap tides in the pioneer marsh was higher than that of spring tides, with the averages being 3.04 ± 2.52 and 1.61 ± 1.60 g L^{-1} ($t = 3.183$, $p < 0.01$). Typhoon Muifa caused a distinct increase in the SSC in the pioneer marsh, with maximum SSCs of 10.37 and 7.62 g l^{-1} before and during landfall, respectively (Fig. 2f). The high SSC persisted for a long period in the pioneer marsh, with its mean values during flood and ebb tides increasing to 3.95 ± 2.64 and 4.55 ± 2.19 g L^{-1}, which were 1.82 and 3.78 times higher than those during spring tides (Fig. 2f; Supporting Information Table S1).

Intertidal hydrodynamics during cold waves in winter

The mean tidal level in the Changjiang Delta was lower in winter than in summer. Inundation depths in the East Chongming Wetland increased during the 2nd cold wave, with maximum water depth in the pioneer and mid marsh reaching 1.96 and 0.93 m, respectively, both of which exceeded the maximum depths (1.84 and 0.86 m) during Typhoon Muifa (Fig. 2a,g,m). The maximum significant wave height ($H_{1/3}$) at the two sites increased to 0.74 and 0.26 m, respectively, during the cold wave (Fig. 2h,n). Although water depth in the pioneer marsh was overall lower in winter compared to summer, the flood and ebb tidal velocities increased, with their maximum speeds rising to 41.0 and 38.8 cm s^{-1}, respectively (Fig. 2i). The mean ebb velocity in the pioneer marsh was higher than the mean flood velocity, which suggests that the tidal current was accelerated after the senescence of salt marsh vegetation (Fig. 3b,c). A comparison of directional shifts in tidal currents in the pioneer marsh further indicates that winter tidal currents were more concentrated (with weaker variation) than those in summer (Supporting Information Fig. S5a,c).

In the winter of 2022, the combined bed shear stress from waves and tidal currents increased significantly, and the duration of high stress extended (Fig. 2e,k). The maximum total bed shear stress in the pioneer marsh during spring tides in December (in the absence of cold waves) increased to 0.34 N m^{-2}, which exceeded the maximum shear stress of 0.21 N m^{-2} during Typhoon Muifa in September. In addition, intertidal SSC in the pioneer marsh did not decrease with lower fluvial sediment inputs, and the minimum of SSC was 1.27 g L^{-1} during spring tides (Fig. 2f,l). In winter, the mean SSC during spring tides was 3.44 ± 1.38 g L^{-1} in flood and 3.69 ± 1.68 g L^{-1} in ebb, both higher than during the summer (2.17 ± 1.93 and 1.18 ± 1.02 g L^{-1}, Fig. 3d,e). Overall, intertidal hydrodynamics in the East Chongming Wetland were enhanced during the winter of 2022, particularly during cold waves, despite lower mean water levels and shallower inundation depths.

Variations in intertidal bed elevation

Storms triggered intertidal bed erosion and deposition. On July 17, 2022, bed elevation ranged from 303.8 cm (at Sta. #1) in the high marsh to 184.4 cm (at Sta. #15) in the pioneer marsh, forming a convex profile (Fig. 4a; Supporting Information Text S7). By September 8, 2022, net accretion occurred from Sta. #4 in the high marsh to the pioneer vegetation; seaward sediment deposits were thicker (Fig. 4a). However, after Typhoon Muifa on September 18, 2022, significant erosion occurred in the high and mid marshes (except for Sta. #7), whereas elevation changes in the low marsh and pioneer zone were smaller and more variable (Fig. 4b).

During the 5 months from summer to winter, the variations in bed elevation in the four zones (high, mid, low, and pioneer marshes) were −2.0, 14.8, 25.0, and 3.6 cm, respectively (Supporting Information Fig. S6a; Supporting Information Table S2). By December 28, the sediment accumulation trend persisted, with the strongest sediment deposition (7.8 and 6.7 cm) detected at Sta. #9 and Sta. #10 in the mid marsh

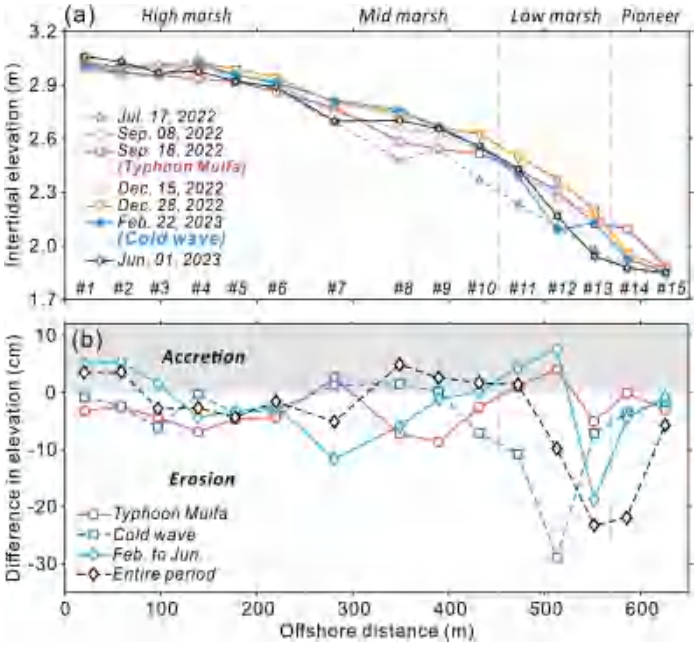

Fig. 4. Variations in bed elevation in the East Chongming Wetland. (a) Elevation changes were derived from seven monthly surveys between July 2022 and June 2023. (b) Transverse variability in bed elevation changes during Typhoon Muifa, cold wave, strong winter waves, and the entire period.

(Fig. 4a). By February 22, 2023, following two cold waves with strong wind waves, 12 of the 15 bed-level monitoring stations experienced net erosion; the strongest erosion occurred at Sta. #12 in the low marsh, reaching 28.8 cm (Fig. 4b). By June 1, 2023, massive bed erosion occurred and the most extensive erosion concentrated at the transition area between the high and mid marsh (Fig. 4b).

Changes in vegetation distribution

Until August 14, 2022, salt marshes expanded uniformly, reaching a total vegetated area of 7.05×10^5 m^2 (Fig. 5a; Supporting Information Text S8). UAV (Unmanned Aerial Vehicle)-based orthorectified imagery shows a distinct alongshore edge between pioneer and low marshes. Strong scouring triggered by Typhoon Muifa resulted in several erosion ponds within the pioneer marsh vegetation, and waves and currents also damaged the aboveground vegetation (Supporting Information Fig. S7a,b). By April 8, 2023, persistent strong wind waves in winter and two cold waves formed two alongshore erosion boundaries (Fig. 5b). The seaward boundary coincided with the former edge between low marsh and pioneer vegetation in summer, corresponding to the strongest erosion (Figs. 4b, 5b). The landward erosion boundary spanned the transition area between mid and low marshes, with damage to vegetation stems and leaves (Supporting Information Fig. S7c–f).

On August 16, 2023, two distinct alongshore bands of salt marsh loss persisted, with the marsh extent reduced by 15.8% to 5.94×10^5 m^2 (Fig. 5c). The seaward marsh loss band was located at the boundary that underwent the strongest erosion in winter (Fig. 5b,c). A landward band of marsh loss appeared in the transition zone between the high and mid marshes, where over 20 cm of erosion occurred from February to June 2023 (Figs. 4b, 5c).

Vegetation coverage and shape index

In August 2022, salt marsh coverage decreased toward the seaward edge, with an average of 0.656 overall (Fig. 6a; Supporting Information Text S9). Vegetation coverage in August 2023 retained a similar pattern, with a significant reduction in the two marsh loss bands; the overall coverage decreased by 15.8% to 0.552% (Fig. 6b). The alongshore statistics in Fig. 6c reveal a large-scale reduction in coverage following successive extreme winter storms and intense wind waves. Meanwhile, from August 2022 to August 2023, the overall marsh LSI rose by 50.8% from 2.183 to 3.292 (Fig. 6d,e). The seaward-most area showed reduced LSI, suggesting that seaward marsh expansion was becoming less fragmented (Fig. 6f).

We extracted variations in marsh coverage and LSI values for cells corresponding to 15 bed-level monitoring stations. Marsh coverage was reduced at almost all stations, with an average reduction of 0.170 (Fig. 7a). Stronger bed erosion was associated with greater marsh coverage loss, with the two variables showing a significant linear correlation ($r = 0.72$, $p = 0.003$) (Fig. 7b). Landscape Shape Index also linearly increased with erosion ($r = 0.63$, $p = 0.011$) (Fig. 7c).

Discussion

Impacts of typhoons

Our results demonstrated that typhoons landing on or passing near the Changjiang Delta can trigger significant impacts on intertidal hydrodynamics and geomorphology of open-coast salt marshes. During extreme typhoons, strong pressure gradients and winds lead to an increase in wave power, while storm surges raise the water level, thereby profoundly altering sediment suspension and transport (Wolf 2009; Needham et al. 2015). The combined effect of waves and surge thus increases intertidal flooding depth, duration, tidal flow speed, and bed shear stress beyond normal meteorological levels (Mariotti et al. 2010). In the open East Chongming Wetland, the total bed shear stress in the pioneer marsh increased during the typhoon events (Fig. 2e), leading to more bed sediment resuspension and increasing SSC in the water column. Q. Zhu et al. (2017) also indicated through field observations that strong winds during storms would increase wave- and current-induced bed shear stress and govern bed-level changes on the open intertidal flats in the Changjiang Delta. In the mid marsh, characterized by relatively low-growing vegetation and fine-grained surficial sediments, the stems and leaves of S. mariqueter failed to fully dissipate waves

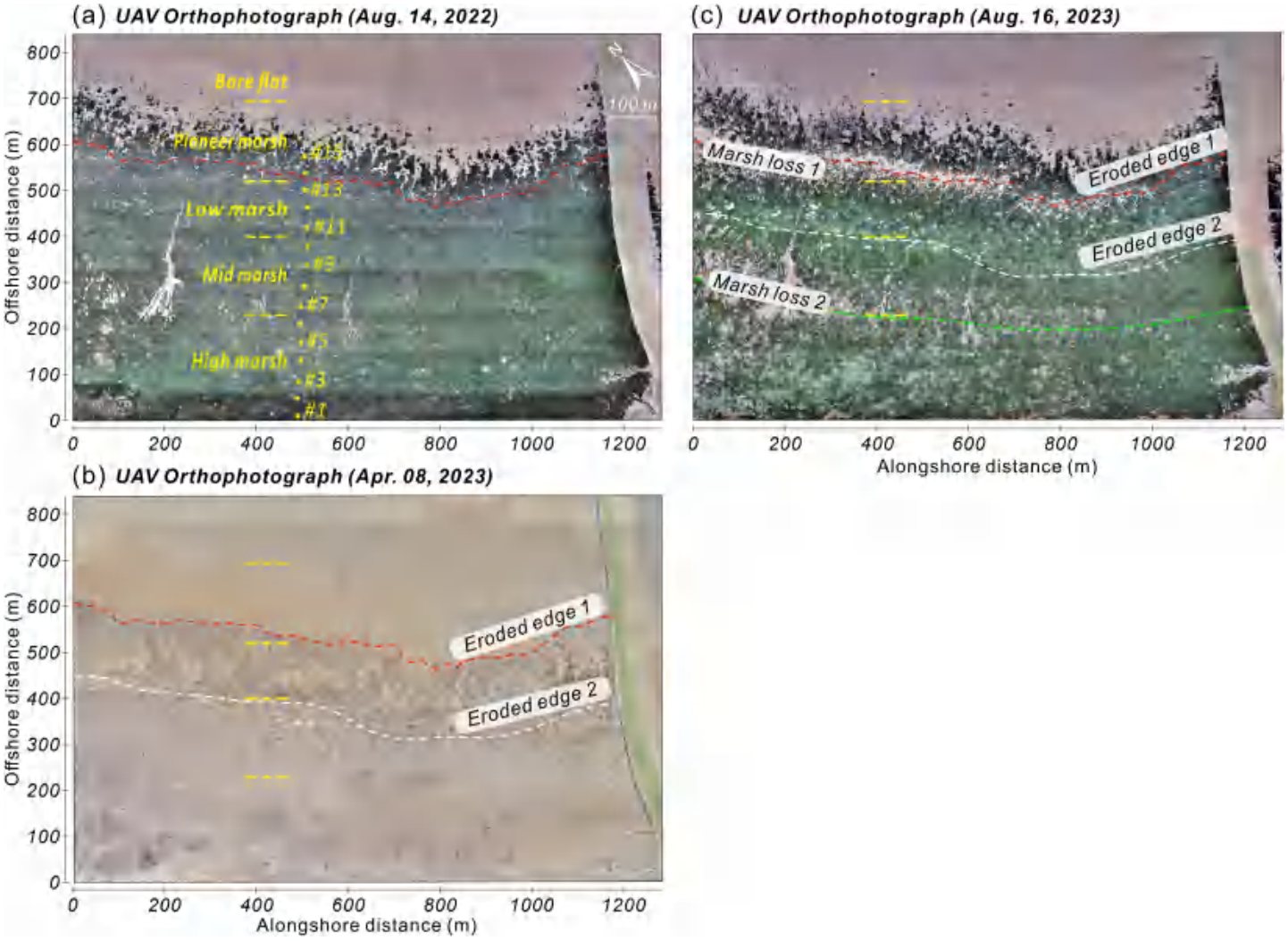

Fig. 5. Vegetation dynamics and geomorphological impact of extreme storms. (a) Unmanned aerial vehicle (UAV)–derived orthophotography of the salt marsh on August 14, 2022, showing the five sub-zones and bed elevation monitoring sites. (b) Post-winter UAV-derived orthophotography on April 8, 2023, reveals widespread die-off and salt marsh degradation, featuring: (i) a pronounced erosional cliff along the pioneer boundary; (ii) a secondary cliff between mid and low marshes; and (iii) extensive and varied-sized erosion ponds between two boundaries. (c) UAV-derived orthophotography on August 16, 2023, showing two distinct bands of salt marsh loss 1 yr later.

and tidal currents, resulting in more erosion of the marsh substrate (Friedrichs and Perry 2001; Fagherazzi and Wiberg 2009). Thus, the mid marsh in the East Chongming Wetland was identified as an erosion hotspot during Typhoon Muifa, which showed a reduction in stem height relative to the high and low marshes (Fig. 4b; Supporting Information Fig. S4).

In addition, the wind-wave attack position during typhoons moved landward with higher tidal levels, the enhanced hydrodynamic forcing triggered low-rigidity salt marshes to break, and thus reduced their resistance in dissipating wave energy and storms (Tonelli et al. 2010; Valentine and Mariotti 2019). Therefore, extensive stands of S. mariqueter in the low and pioneer marshes collapsed under the scouring effects of waves and tidal currents during the typhoon, forming extensive erosion ponds and cliffs (Supporting Information Fig. S7a,b; Fig. 8a,b).

Such intense and uneven intertidal erosion, triggered by severe summer typhoons, profoundly reshaped the short-term eco-morphodynamic equilibria of the tidal wetlands, driving them to deviate from their prior growth trajectory. Although some of the eroded areas experienced accretion after the typhoon, this does not mean salt marsh systems can fully recover to their pre-damage state (Fig. 4a). Our study highlighted an often-overlooked process: direct damage to salt marsh stems and leaves caused by extreme typhoons with fast flows and strong waves (Callaghan et al. 2010; Rupprecht et al. 2017). The open-coast East Chongming Wetland is colonized by native S. mariqueter, the stems of which have low

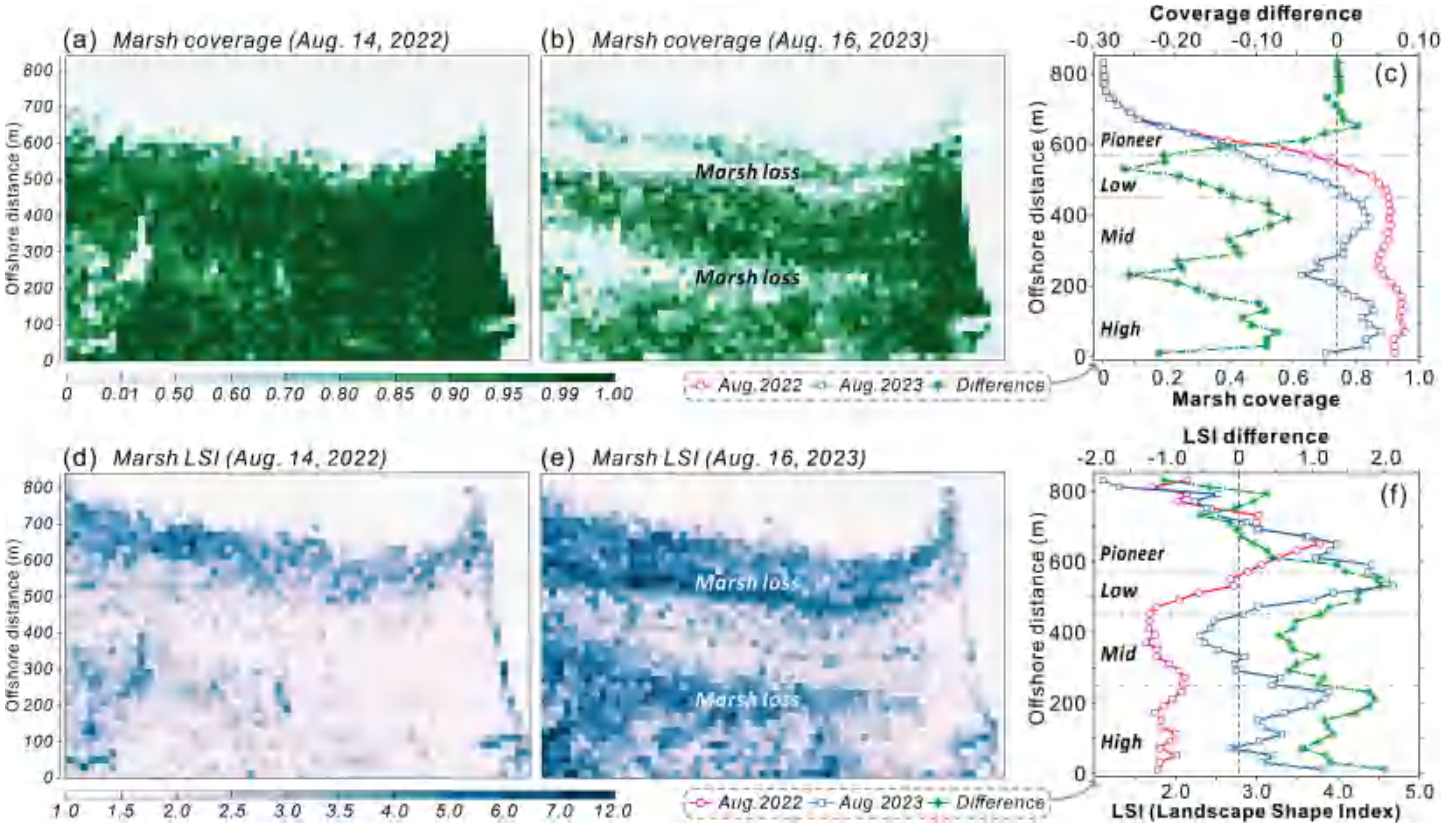

Fig. 6. Grid-scale changes in salt marsh coverage and Landscape Shape Index (LSI). (a, b) Fraction of vegetated area (i.e., salt marsh coverage) in August 2022 and August 2023. Two distinct bands of salt marsh loss correspond spatially to areas of strong bed erosion during winter 2022 (Fig. 5c). (c) Alongshore-averaged marsh coverage in August 2022 (red) and August 2023 (blue), and the difference between the two (green). (d, e) The LSI of the salt marsh (i.e., the marsh perimeter/area ratio within a cell) quantifies marsh boundary complexity in August 2022 and August 2023. (f) The alongshore-averaged LSI with interannual difference.

flexural strength and are easily broken by strong hydrodynamic forces; once the stem breaks, the plant's physiological functions partially collapse within a short period (Ge et al. 2019; Yuan et al. 2020). In addition, after the intertidal substrate is eroded, the plant's subsurface roots and rhizomes can also be damaged, making regeneration after the storms difficult. Even if the salt marsh partly recovers, its ability to reduce waves and tides will not return to pre-typhoon levels.

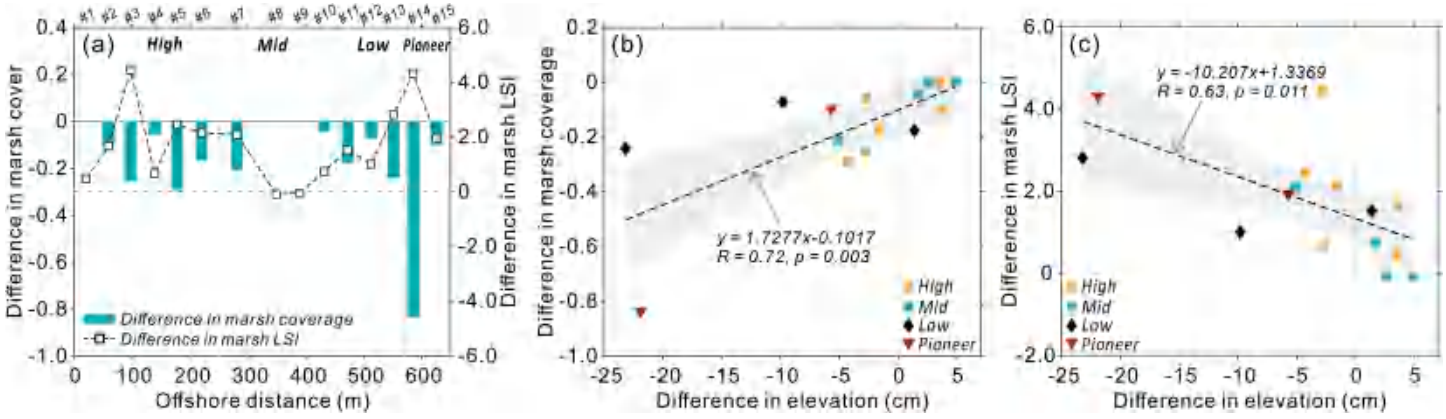

Fig. 7. (a) Transverse variation in salt marsh coverage and Landscape Shape Index (LSI) across grids spatially coincident with the 15-bed elevation monitoring sites. (b, c) Relationships between bed elevation change and variations in marsh coverage and LSI.

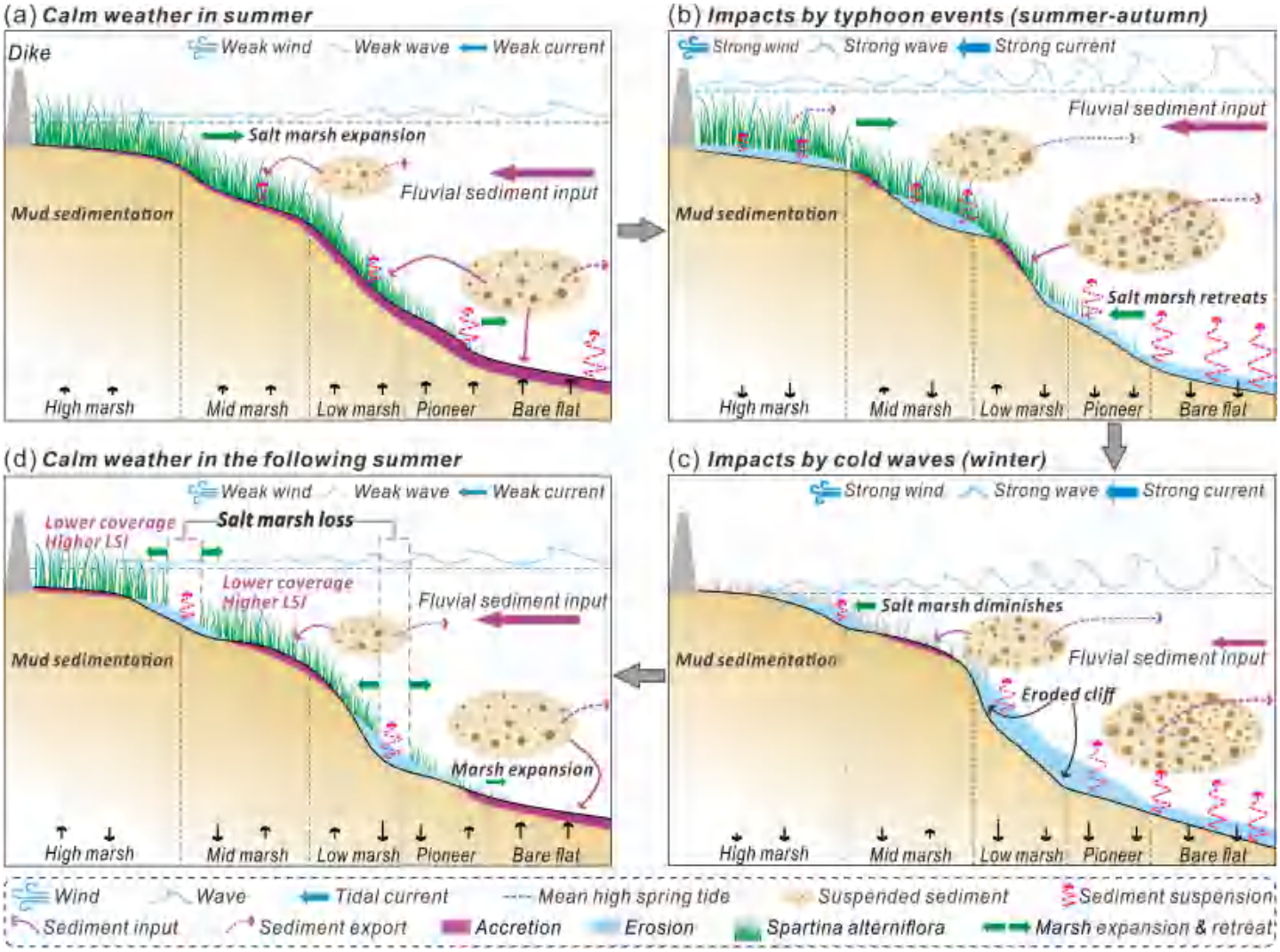

Fig. 8. Conceptual diagram of the eco-morphodynamic response of salt marshes to successive extreme storms in the East Chongming Wetland. (a) Calm summer conditions: Sediments deposit across bare flats and salt marshes, contributing to intertidal accretion and marsh expansion. (b) Typhoon phase: Enhanced combined wave-current bed shear stresses generate net large-scale sediment erosion and export, while stronger hydrodynamic scouring triggers retreat of the marsh edge. (c) Winter disturbance: Salt marsh die-off combines with higher bed shear stresses during cold waves, producing erosional marsh cliffs, ponds, and steepened intertidal profiles. (d) Recovery phase: Incomplete marsh recovery at prior erosion hotspots creates marsh loss bands. Overall, successive storms reduce system-wide recovery capability, compromising ecological services and geomorphic stability of deltaic tidal wetlands.

Thus, the 1st typhoon not only induced direct intertidal substrate erosion but also heightened the vulnerability of the intertidal salt marsh ecosystem to subsequent threats. Approximately 3–4 typhoons strike the Changjiang Delta each year (Yun 2004). Their frequency is expected to increase with global climate change, as typhoon tracks gradually shift landward and poleward along the East China coast (Xu et al. 2024). Overall, the degradation of salt marsh functions induced by extreme typhoons in summer can pose substantial risks to the medium- and long-term effectiveness and sustainability of coastal nature-based solutions (Supporting Information Fig. S8).

It should be pointed out that sheltered salt marshes (e.g., in the Venice Lagoon, Wadden Sea, Virginia Coast Reserve, and San Francisco Bay) are protected by natural barriers or artificial structures, with storm wave energy effectively dissipated before reaching the marsh interior. In these systems, storm surges, therefore, deliver abundant sediment to the marsh interior, promoting net vertical accretion and enhancing the role of marshes as net sediment sinks during storm events (Turner et al. 2006; Q. Zhu and Wiberg 2022; Tognin et al. 2025). In contrast, narrow and open-coast deltaic salt marshes, like the area studied herein in the Changjiang Delta, lack adequate protection from storm impacts. Successive

storms can trigger severe bed erosion and salt marsh deterioration, weakening the post-storm recovery of marsh vegetation and degrading intertidal ecological functions and geomorphic stability.

Impacts of cold waves on intertidal morphology

Winter cold waves intensify bed erosion in intertidal areas lacking salt marsh vegetation protection. Although the mean sea level in the East China Sea drops in winter, the strong onshore winds during cold waves can trigger significant storm surges, increasing coastal water depths and wave energy (Kim et al. 2020). Consequently, the combination of storm surge and enhanced wave shear stresses can lead to localized marsh erosion (Coulombier et al. 2012). Crucially, salt marshes senescence in winter, with a large decrease in aboveground biomass in the East Chongming Wetland (Supporting Information Fig. S7c–f). As a result, flood and ebb tidal currents are no longer attenuated or delayed by the marsh vegetation, and wave dissipation is also reduced in the absence of stems and leaves (Callaghan et al. 2010). The combined effects of elevated water levels, intensified wave and tidal currents, and the absence of aboveground marsh vegetation led to large-scale erosion of fine-grained intertidal bed sediments (Fig. 4b). Our results clearly showed the formation of eroded cliffs and ponds along the low marsh edge, areas that were previously colonized during the summer (Figs. 5b, 8c). These findings suggest that cold waves enhance the erodibility of open deltaic tidal flat systems in winter by altering intertidal hydrodynamics and removing the protective buffer of vegetation (WinklerPrins et al. 2024). This effect is particularly pronounced in vulnerable low marsh areas exposed to stronger wind waves.

Cold waves damage intertidal systems not only through physical erosion (Fig. 8e) but also via freeze–thaw cycles. These sudden temperature drops can produce ice rafts that mobilize sediments (Nordio and Fagherazzi 2023) and harm vegetation roots, potentially affecting their medium- and long-term growth and health (Zhao et al. 2022). During the two cold waves in January 2023, offshore temperatures in the East Chongming Wetland dropped sharply by 11.0°C and 9.9°C, respectively, over a 24-h period, and inland lowest temperatures reached −8°C. In the high and mid intertidal zones, the sharp cooling caused the pore water of the sediments to freeze rapidly, destroying the adhesion between the sediment particles (Woodin et al. 2010; Inamdar et al. 2018). Freezing and thawing also resulted in immediate physical damage to salt marsh roots, impairing subsurface tissue and even leading to irreversible death (Elmer et al. 2013; Bhattacharya 2022). Salt marsh roots were exposed to high-energy hydrodynamic conditions during the cold wave, further reducing the ability to anchor to intertidal substrates (Coulombier et al. 2012; Kim et al. 2020).

Thus, the intertidal bed sediments of the open East Chongming Wetland experienced a significant increase in net erosion in response to multiple cold waves (Fig. 8c). In particular, if marsh subsurface roots are extensively damaged or washed away during winter, marsh recovery in the following spring would be greatly impeded (Fig. 8d).

Cascading effects of extreme storms

Successive extreme typhoons and cold waves occurred in the Changjiang Delta in 2022, damaging both the surface and subsurface components of salt marshes in the open East Chongming Wetland, with impacts on their ecosystem structure extending far beyond those of a single storm. Despite the relatively short duration of each extreme hydroclimatic event, the cascading effects of their hydromechanical and biological impacts can accumulate in terms of damage to intertidal salt marsh vegetation (Fig. 8) (Cahoon 2006; Morton and Barras 2011; Leonardi et al. 2018). The combined wave-current shear stresses during typhoons not only eroded surficial sediments but also directly caused vegetation stems/leaves to fold and break, impairing plant growth over time (Fagherazzi and Wiberg 2009; Rupprecht et al. 2017; Temmerman et al. 2023). Subsequent cold waves in winter induced intense hydrodynamics that exacerbated erosion of unvegetated flats, while abrupt cooling and freeze–thaw processes likely altered intertidal sediment structure and freeze subsurface marsh roots (Coulombier et al. 2012; WinklerPrins et al. 2024). This sequential damage of the tidal marsh vegetation across seasons might impair the health and wave-attenuating capacity of the salt marshes (Ge et al. 2019; Wang et al. 2024). If these disturbances are too frequent, deltaic salt marshes may shift from recovery to decline (Kirwan and Megonigal 2013; Fagherazzi et al. 2020).

Climate change is globally increasing the frequency and intensity of extreme hydrometeorological events in densely populated river deltas, such as the Changjiang, Yellow, Mekong, and Mississippi deltas (van de Vijsel et al. 2024), and the cascading effects of multiple coastal storms pose serious threats to marsh resilience (Leonardi et al. 2018). At the same time, reduced fluvial sediment supply and rising sea levels further jeopardize salt marshes' stability (Friedrichs and Perry 2001; Schuerch et al. 2018; Murray et al. 2022). The combined effect of these stressors poses an unprecedented and urgent threat to the effectiveness and sustainability of gray-green coastal infrastructure and nature-based solutions that rely on salt marsh ecological functions (Z. Zhu et al. 2020; Temmerman et al. 2023). Our results show that the risk of coastal land erosion in the East Chongming Wetland is significantly increased during extreme storm events, and the native S. mariqueter is more sensitive to storm hydrodynamics, making it prone to loss. The total vegetated area has decreased by 15.8% in our study period, and marsh distribution is becoming more fragmented, with the formation of two alongshore bands of salt marsh loss (Figs. 5, 6).

Our 2024 data, collected 2 yr after extreme Typhoons Hinnamnor and Muifa in the summer of 2022, reveal a

distinct mismatch between intertidal sedimentation and marsh vegetation recovery. Despite post-storm sediment accretion, damaged vegetation between the high and mid marsh has not completely recovered, displaying persistent non-vegetated patches and indicating that storms have a long-term adverse impact (Supporting Information Figs. S9, S10). Therefore, this study highlights that the recovery capability of an impaired salt marsh system is largely dependent on sediment availability and the frequency of successive extreme storms. Storms may act as a critical triggering perturbation, while adequate sediment supply can effectively buffer and offset storm-induced geomorphic and ecological impacts (Stagg and Mendelssohn 2011; Yang et al. 2020; Dzimballa et al. 2025). If successive storms, coupled with other external stressors (sea level rise, dredging, and reclamations, etc.), surpass the marsh ecosystem's self-repair threshold, they are highly likely to induce irreversible or long-term degradation of salt marsh vegetation (Cahoon 2006; Leonardi et al. 2018; Hu et al. 2025).

It should also be emphasized that species-specific functional traits strongly modulate salt marshes' eco-morphodynamic responses and post-storm recovery. Salt marsh species, with rigid stems and leaves, such as Spartina alterni*fl*ora, can effectively withstand strong intertidal hydrodynamics during extreme coastal storms and exhibit rapid recovery post-disturbance (Rupprecht et al. 2017). The short and flexible native S. mariqueter shows far weaker turbulence attenuation, sediment retention, and bed erosion resistance than the rigid invasive S. alterni*fl*ora and high-elevation native Phragmites australis. Thus, S. alterni*fl*ora removal along the Chinese coast will trigger short-term declines in nature-based storm defense, exacerbating storm-driven erosion in exposed and sediment-starved deltaic wetlands (Wu et al. 2025; Liu et al. 2026).

Our findings overall reveal that successive typhoons in summer-autumn and cold waves in winter drastically heighten the risk of destabilization for intertidal marshes' ecological defenses, possibly affecting the dikes in the Changjiang Delta (Fig. 8e). In open-coast salt marshes in the East Chongming Wetland, successive extreme storms, compounded with reduced riverine sediment supply, sea level rise, and narrowing salt marshes, intensify dike-front erosion, surge water levels, and dike failure risks (Yuan et al. 2020; Wei et al. 2022; Murray et al. 2022; Shi et al. 2025). Conversely, dikes can alter the hydrodynamics in front of the marsh, exacerbating intertidal bed erosion and restricting landward migration and growth of salt marsh vegetation (Schuerch et al. 2018; Yang et al. 2020). If marsh vegetation degradation or die-off reduces the system's wave-dissipation capacity below the levels required for ecological dike design, the intertidal system will be subjected to stronger hydrodynamic conditions and greater flooding risks (Borsje et al. 2011; Temmerman et al. 2023). Therefore, understanding intertidal hydrodynamics, sediment budgets, bed elevation changes, and vegetation dynamics is essential for designing effective nature-based solutions to address future climatic extremes and mitigate coastal hazards (Temmerman et al. 2023; Dzimballa et al. 2025). Failing to account for extreme storm damage to salt marshes may lead to underestimating the vulnerability of these solutions under sea-level rise. To address this, climate-adaptive strategies tailored to local hydro-sedimentary conditions and key risks are urgently needed, especially in densely populated mega-deltas (Chan et al. 2024; van de Vijsel et al. 2024; Wang et al. 2025). This study has certain limitations. Longer-term monitoring datasets are needed to further examine the eco-morphodynamic responses of open, sheltered, and restored tidal wetlands (after invasive species removal) to extreme storms.

Author Contributions

Jie Wang: investigation, methodology, data curation, formal analysis, writing – original draft, writing – review and editing. Ming Shi: investigation, methodology, data curation. Zhijun Dai: conceptualization, investigation, supervision, project administration, funding acquisition, writing – original draft, writing – review and editing. Huan-Feng Duan: methodology, investigation. Xuefei Mei: methodology, investigation. Wen Wei: investigation. Jiejun Luo: data curation, methodology. Weihua Li: formal analysis investigation. Sergio Fagherazzi: data curation, formal analysis, writing – review and editing.

Acknowledgments

This study was supported by the National Natural Science Key Foundation of China (42430406), Shanghai International Science and Technology Cooperation Fund Project (23230713800, 23590780200, 24230740100), and the Funds for the Ministry of Science and Technology of China (SKLEC). Sergio Fagherazzi was partly funded by the US National Science Foundation awards 2224608 (PIE LTER) and 2425178 (VCR LTER).

Con*fl*icts of Interest

None declared.

Data Availability Statement

Data are available on request from the authors.

References

Bendoni, M., R. Mel, L. Solari, S. Lanzoni, S. Francalanci, and H. Oumeraci. 2016. "Insights into Lateral Marsh Retreat Mechanism through Localized Field Measurements." Water Resources Research 52: 1446–1464. https://doi.org/10.1002/2015WR017966.

Bhattacharya, A. 2022. "Effect of Low-Temperature Stress on Germination, Growth, and Phenology of Plants: A Review." In Physiological Processes in Plants Under Low Temperature

Stress. Springer. https://doi.org/10.1007/978-981-16-9037-2_1.

Borsje, B. W., B. K. van Wesenbeeck, F. Dekker, et al. 2011. "How Ecological Engineering Can Serve in Coastal Protection." Ecological Engineering 37, no. 2: 113–122. https://doi.org/10.1016/j.ecoleng.2010.11.027.

Cahoon, D. R. 2006. "A Review of Major Storm Impacts on Coastal Wetland Elevations." Estuaries and Coasts 29: 889–898. https://doi.org/10.1007/BF02798648.

Callaghan, D. P., T. J. Bouma, P. Klaassen, D. Van Der Wal, M. J. F. Stive, and P. M. J. Herman. 2010. "Hydrodynamic Forcing on Salt-Marsh Development: Distinguishing the Relative Importance of Waves and Tidal Flows." Estuarine, Coastal and Shelf Science 89: 73–88. https://doi.org/10.1016/j.ecss.2010.05.013.

Chan, F. K. S., A. Paszkowski, Z. Wang, et al. 2024. "Building Resilience in Asian Mega-Deltas." Nature Reviews Earth & Environment 5, no. 7: 522–537. https://doi.org/10.1038/s43017-024-00561-x.

Chen, J. Y., H. T. Shen, and C. X. Yun. 1988. Hydrodynamics and Geomorphic Evolution in the Yangtze (Changjiang) Estuary. Shanghai Science and Technology Press (in Chinese).

Coulombier, T., U. Neumeier, and P. Bernatchez. 2012. "Sediment Transport in a Cold Climate Salt Marsh (St. Lawrence Estuary, Canada), the Importance of Vegetation and Waves." Estuarine, Coastal and Shelf Science 101: 64–75. https://doi.org/10.1016/j.ecss.2012.02.014.

Dai, Z., X. Mei, S. E. Darby, Y. Lou, and W. Li. 2018. "Fluvial Sediment Transfer in the Changjiang (Yangtze) River-Estuary Depositional System." Journal of Hydrology 566: 719–734. https://doi.org/10.1016/j.jhydrol.2018.09.019.

Dethier, E. N., C. E. Renshaw, and F. J. Magilligan. 2022. "Rapid Changes to Global River Suspended Sediment Flux by Humans." Science 376: 1447–1452. https://doi.org/10.1126/science.abn7980.

Dzimballa, S., P. W. J. M. Willemsen, V. Kitsikoudis, B. W. Borsje, and D. C. M. Augustijn. 2025. "Numerical Modelling of Biogeomorphological Processes in Salt Marsh Development: Do Short-Term Vegetation Dynamics Influence Long-Term Development?" Geomorphology 471: 109534. https://doi.org/10.1016/j.geomorph.2024.109534.

Elmer, W. H., S. Useman, R. W. Schneider, et al. 2013. "Sudden Vegetation Dieback in Atlantic and Gulf Coast Salt Marshes." Plant Disease 97, no. 4: 436–445. https://doi.org/10.1094/PDIS-09-12-0871-FE.

Fagherazzi, S., G. Mariotti, N. Leonardi, A. Canestrelli, W. Nardin, and W. S. Kearney. 2020. "Salt Marsh Dynamics in a Period of Accelerated Sea Level Rise." Journal of Geophysical Research: Earth Surface 125, no. 8: e2019JF005200. https://doi.org/10.1029/2019JF005200.

Fagherazzi, S., and P. L. Wiberg. 2009. "Importance of Wind Conditions, Fetch, and Water Levels on Wave-Generated Shear Stresses in Shallow Intertidal Basins." Journal of Geophysical Research: Earth Surface 114: F03022. https://doi.org/10.1029/2008JF001139.

Friedrichs, C. T., and J. E. Perry. 2001. "Tidal Salt Marsh Morphodynamics: A Synthesis." Journal of Coastal Research 27: 7–37 https://www.jstor.org/stable/25736162.

Ge, Z. M., S. H. Li, L. S. Tan, Y. L. Li, and Z. J. Hu. 2019. "The Importance of the Propagule-Sediment-Tide "Power Balance" for Revegetation at the Coastal Frontier." Ecological Applications 29, no. 7: e01967. https://doi.org/10.1002/eap.1967.

Hu, Y., L. Gong, Y. Song, et al. 2025. "Synergistic Effects of Elevation Loss and Environmental Extremes Trigger Salt Marsh Die-off in the Yangtze Estuary." Ocean and Coastal Management 270: 107882. https://doi.org/10.1016/j.ocecoaman.2025.107882.

Inamdar, S., E. Johnson, R. Rowland, D. Warner, R. Walter, and D. Merritts. 2018. "Freeze-Thaw Processes and Intense Rainfall: The One-Two Punch for High Sediment and Nutrient Loads from Mid-Atlantic Watersheds." Biogeochemistry 141, no. 3: 333–349. https://doi.org/10.1007/s10533-017-0417-7.

Kim, J. Y., J. Kaihatu, K. A. Chang, S. H. Sun, T. P. Huff, and R. A. Feagin. 2020. "Effect of Cold Front-Induced Waves along Wetlands Boundaries." Journal of Geophysical Research: Oceans 125, no. 12: e2020JC016603. https://doi.org/10.1029/2020JC016603.

Kirwan, M. L., and J. P. Megonigal. 2013. "Tidal Wetland Stability in the Face of Human Impacts and Sea-Level Rise." Nature 504, no. 7478: 53–60. https://doi.org/10.1038/nature12856.

Leonardi, N., I. Carnacina, C. Donatelli, et al. 2018. "Dynamic Interactions between Coastal Storms and Salt Marshes: A Review." Geomorphology 301: 92–107. https://doi.org/10.1016/j.geomorph.2017.11.001.

Li, X., L. Ren, Y. Liu, C. Craft, Ü. Mander, and S. Yang. 2014. "The Impact of the Change in Vegetation Structure on the Ecological Functions of Salt Marshes: The Example of the Yangtze Estuary." Regional Environmental Change 14, no. 2: 623–632. https://doi.org/10.1007/s10113-013-0520-9.

Liang, X. X., Z. J. Dai, H. Huang, et al. 2024. "Elevation Inversion of Mangrove Tidal Flat Geomorphology Based on UAV Aerial Survey. Advances in Marine." Science 42, no. 2: 384–399 (in Chinese with English abstract) 10.12362/j.issn.1671-6647.20230215001.

Liu, B., C. Thompson, Z. Zhou, et al. 2026. "Differences in Turbulence Dissipation and Sediment Retention Shape the Coastal Protection Capacity of Native and Exotic Saltmarsh Species." Limnology and Oceanography 71, no. 2: e70338. https://doi.org/10.1002/lno.70338.

Mariotti, G., S. Fagherazzi, P. L. Wiberg, K. J. McGlathery, L. Carniello, and A. Defina. 2010. "Influence of Storm Surges and Sea Level on Shallow Tidal Basin Erosive Processes." Journal of Geophysical Research: Oceans 115: C11012. https://doi.org/10.1029/2009JC005892.

Mei, X., N. Leonardi, J. Dai, and J. Wang. 2023. "Cellular Automata to Understand the Prograding Limit of Deltaic Tidal Flat." Engineering Applications of Computational Fluid Mechanics 17, no. 1: 2234038. https://doi.org/10.1080/19942060.2023.2234038.

Morton, R. A., and J. A. Barras. 2011. "Hurricane Impacts on Coastal Wetlands: A Half-Century Record of Storm-Generated Features from Southern Louisiana." Journal of Coastal Research 275: 27–43. https://doi.org/10.2112/jcoastres-d-10-00185.1.

Murray, N. J., T. A. Worthington, P. Bunting, et al. 2022. "High-Resolution Mapping of Losses and Gains of Earth's Tidal Wetlands." Science 376, no. 6594: 744–749. https://doi.org/10.1126/science.abm9583.

Needham, H. F., B. D. Keim, and D. Sathiaraj. 2015. "A Review of Tropical Cyclone-Generated Storm Surges: Global Data Sources, Observations, and Impacts." Reviews of Geophysics 53, no. 2: 545–591. https://doi.org/10.1002/2014RG000477.

Nordio, G., and S. Fagherazzi. 2023. "Recovery of Salt Marsh Vegetation after Ice-Rafting." Marine Ecology Progress Series 710: 57–70. https://doi.org/10.3354/meps14294.

Remmel, T. K., and F. Csillag. 2003. "When Are Two Landscape Pattern Indices Significantly Different?" Journal of Geographical Systems 5: 331–351. https://doi.org/10.1007/s10109-003-0116-x.

Rupprecht, F., I. Möller, M. Paul, et al. 2017. "Vegetation-Wave Interactions in Salt Marshes under Storm Surge Conditions." Ecological Engineering 100: 301–315. https://doi.org/10.1016/j.ecoleng.2016.12.030.

Schuerch, M., T. Spencer, S. Temmerman, et al. 2018. "Future Response of Global Coastal Wetlands to Sea-Level Rise." Nature 561, no. 7722: 231–234. https://doi.org/10.1038/s41586-018-0476-5.

Shi, M., Z. Dai, J. Luo, et al. 2025. "Wave Attenuation over a Scirpus Mariqueter Salt Marsh During Typhoon Muifa." Estuarine, Coastal and Shelf Science 315: 109155. https://doi.org/10.1016/j.ecss.2025.109155.

Silvestri, S., A. Defina, and M. Marani. 2005. "Tidal Regime, Salinity and Salt Marsh Plant Zonation." Estuarine, Coastal and Shelf Science 62, no. 1–2: 119–130. https://doi.org/10.1016/j.ecss.2004.08.010.

Soulsby, R. L. 1995. "Bed Shear-Stress Due to Combined Waves and Currents." In Advances in Coastal Morphodynamics, edited by M. J. F. Stive, H. J. de Vriend, J. Fredsøe, et al., 4–23. Delft Hydraulics.

Soulsby, R. L., and S. Clarke. 2005. Bed Shear-Stresses Under Combined Waves and Currents on Smooth and Rough Beds. Report TR137. HR Wallingford.

Stagg, C. L., and I. A. Mendelssohn. 2011. "Controls on Resilience and Stability in a Sediment-Subsidized Salt Marsh." Ecological Applications 21: 1731–1744. https://doi.org/10.1890/09-2128.1.

Temmerman, S., E. M. Horstman, K. W. Krauss, J. C. Mullarney, I. Pelckmans, and K. Schoutens. 2023. "Marshes and Mangroves as Nature-Based Coastal Storm Buffers." Annual Review of Marine Science 15, no. 1: 95–118. https://doi.org/10.1146/annurev-marine-040422-092951.

Tognin, D., A. D'Alpaos, M. Ghinassi, and L. Carniello. 2025. "Marsh Topography Reveals the Signature of Storm-Surge-Driven Sedimentation." Geology 53, no. 1: 45–49. https://doi.org/10.1130/G52552.1.

Tonelli, M., S. Fagherazzi, and M. Petti. 2010. "Modeling Wave Impact on Salt Marsh Boundaries." Journal of Geophysical Research: Oceans 115: C09028. https://doi.org/10.1029/2009JC006026.

Turner, R. E., J. J. Baustian, E. M. Swenson, and J. S. Spicer. 2006. "Wetland Sedimentation from Hurricanes Katrina and Rita." Science 314, no. 5798: 449–452. https://doi.org/10.1126/science.1129116.

Valentine, K., and G. Mariotti. 2019. "Wind-Driven Water Level Fluctuations Drive Marsh Edge Erosion Variability in Microtidal Coastal Bays." Continental Shelf Research 176: 76–89. https://doi.org/10.1016/j.csr.2019.03.002.

van de Vijsel, R. C., M. Scheffer, and A. J. Hoitink. 2024. "Tipping Points in River Deltas." Nature Reviews Earth & Environment 5, no. 12: 843–858. https://doi.org/10.1038/s43017-024-00610-5.

van Rijn, L. C. 1993. Principles of Sediment Transport in Rivers, Estuaries and Coastal Seas. Amsterdam, the Netherlands: Aqua Publications.

Wang, J., Z. Dai, S. Fagherazzi, Y. Lou, X. Mei, and B. Ma. 2024. "Large-Scale Sedimentary Shift Induced by a Mega-Dam in Deltaic Flats." Sedimentology 71, no. 4: 1084–1112. https://doi.org/10.1111/sed.13168.

Wang, J., Z. Dai, X. Mei, H. F. Duan, and J. H. Nienhuis. 2025. "Response Time of Global Deltas to Changes in Fluvial Sediment Supply." Nature Communications 16, no. 1: 5573. https://doi.org/10.1038/s41467-025-60531-9.

Wei, W., Z. Dai, W. Pang, J. Wang, Y. Chen, and S. Gao. 2022. "Frequency-Dependent Wave Damping by Tidal Wetlands Under Storm Conditions." Journal of Hydrology 613: 128415. https://doi.org/10.1016/j.jhydrol.2022.128415.

Whitehouse, R. 2000. Dynamics of Estuarine Muds. Thomas Telford. https://doi.org/10.1680/doem.28647.

Willemsen, P. W. J. M., B. P. Smits, B. W. Borsje, et al. 2022. "Modeling Decadal Salt Marsh Development: Variability of the Salt Marsh Edge under Influence of Waves and Sediment Availability." Water Resources Research 58, no. 1: e2020WR028962. https://doi.org/10.1029/2020WR028962.

WinklerPrins, L., J. R. Lacy, M. T. Stacey, J. B. Logan, and A. W. Stevens. 2024. "Seasonality of Retreat Rate of a Wave-Exposed Marsh Edge." Journal of Geophysical Research: Earth Surface 129, no. 7: e2023JF007468. https://doi.org/10.1029/2023JF007468.

Wolf, J. 2009. "Coastal Flooding: Impacts of Coupled Wave-Surge-Tide Models." Natural Hazards 49, no. 2: 241–260. https://doi.org/10.1007/s11069-008-9316-5.

Woodin, S. A., D. S. Wethey, and N. Volkenborn. 2010. "Infaunal Hydraulic Ecosystem Engineers: Cast of Characters and Impacts." Integrative and Comparative Biology 50, no. 2: 176–187 https://www.jstor.org/stable/40793141.

Wu, Y., Z. Zhou, C. Dong, et al. 2025. "Impacts of Exotic Saltmarsh Vegetation Removal and Native Saltmarsh Vegetation Restoration on Bed Level Change and Surficial Sediment Distribution in an Estuary Wetland." Journal of Geophysical Research: Earth Surface 130, no. 7: e2024JF008119. https://doi.org/10.1029/2024JF008119.

Xu, C., Y. Yang, J. Jia, J. D. Bricker, and Y. P. Wang. 2024. "A 70-Year Record Reveals the Poleward Shift of Tropical Cyclone Tracks in the East China Coastal Ocean Is Twice that of Landward Shift." Global and Planetary Change 242: 104566. https://doi.org/10.1016/j.gloplacha.2024.104566.

Yang, S. L., X. Luo, S. Temmerman, et al. 2020. "Role of Delta-Front Erosion in Sustaining Salt Marshes under Sea-Level Rise and Fluvial Sediment Decline." Limnology and Oceanography 65, no. 9: 1990–2009. https://doi.org/10.1002/lno.11432.

Yuan, L., Y. H. Chen, H. Wang, et al. 2020. "Windows of Opportunity for Salt Marsh Establishment: The Importance for Salt Marsh Restoration in the Yangtze Estuary." Ecosphere 11, no. 7: e03180. https://doi.org/10.1002/ecs2.3180.

Yun, C. X. 2004. Basic Law of the Recent Evolution of the Changjiang Estuary. China Ocean Press (in Chinese).

Zhao, K., G. Coco, Z. Gong, et al. 2022. "A Review on Bank Retreat: Mechanisms, Observations, and Modeling." Reviews of Geophysics 60, no. 2: e2021RG000761. https://doi.org/10.1029/2021RG000761.

Zhu, Q., B. C. Van Prooijen, Z. B. Wang, and S. L. Yang. 2017. "Bed-Level Changes on Intertidal Wetland in Response to Waves and Tides: A Case Study from the Yangtze River Delta." Marine Geology 385: 160–172. https://doi.org/10.1016/j.margeo.2017.01.003.

Zhu, Q., and P. L. Wiberg. 2022. "The Importance of Storm Surge for Sediment Delivery to Microtidal Marshes." Journal of Geophysical Research: Earth Surface 127, no. 9: e2022JF006612. https://doi.org/10.1029/2022JF006612.

Zhu, Z., V. Vuik, P. J. Visser, et al. 2020. "Historic Storms and the Hidden Value of Coastal Wetlands for Nature-Based Flood Defence." Nature Sustainability 3, no. 10: 853–862. https://doi.org/10.1038/s41893-020-0556-z.

Supporting Information

Additional Supporting Information may be found in the online version of this article.

Submitted 10 September 2025
Revised 23 March 2026
Accepted 12 June 2026